Advances in Research

22(2): 12-27, 2021; Article no.AIR.66731
ISSN: 2348-0394, NLM ID: 101666096

Design and Optimise a GARField MRI Resonator

A. Muhammad[1*], M. D. Oladipupo[1], I. K. Suleiman[1] and O. L. Jane[2]

[1]*Department of Physics, Ibrahim Badamasi Babangida University, Lapai, Nigeria.*
[2]*Department of Geophysics, Federal University of Technology, Minna, Nigeria.*

Authors' contributions

This work was carried out in collaboration among all authors. All authors read and approved the final manuscript.

Article Information

DOI: 10.9734/AIR/2021/v22i230294
Editor(s):
(1) Dr. José Alberto Duarte Moller, Center for Advanced Materials Research, Mexico.
Reviewers:
(1) H. Sheik Mujibur Rahman, Jamal Mohamed College, India.
(2) Ramjeet Singh Yadav, Ashoka Institute of Technology and Management, India.
Complete Peer review History: http://www.sdiarticle4.com/review-history/66731

Original Research Article

Received 01 February 2021
Accepted 07 April 2021
Published 29 April 2021

ABSTRACT

The design of a Nuclear Magnetic Resonance (NMR) sensor coil for a GARField NMR system was examined. The target design has a diameter about $10 - 20$ mm and length $5 - 15$ mm tuned to frequency of $22 - 23.4$ MHz at 50 Ω total impedance. Nine different sets of coils were built with different numbers of turns (3, 5, and 7) and different thickness of wire to vary the wire resistance. The report was to examine based on the design parameters the best resonant circuit for a GARField MRI system. The acquired tuning characteristics from these resonant circuits were interpreted using MATLAB scripts and Excel spreadsheet to compare each coil with already existing theory of resonators. This was achieved by matching each resonant circuit using a match and tuning capacitor to the required frequency (22-23.4 MHz) and to 50 Ω total impedance at resonance. It was found that there is no easy method to estimate the inductance of the coil of wire. The result for the experimental inductance was found to be 0.5 μF and resistance of 0.4 Ω for a medium coil of wire with 5 numbers of turns, diameter of 0.45 and length of 0.7 mm. The initial attempt to fit the experimental data to that of the theory failed due to the absence of stray capacitance in the theory. However, when stray capacitor with value ranging between $30 - 40$ pF was incorporated in parallel with the tank circuit, it was found that both the experiment and theory fit as expected.
Three coils were tested in the NMR laboratory using a GARField spectrometer to examine the best

**Corresponding author: E-mail: kaleabdullahi75@gmail.com;*

coil that will be suitable for NMR experiment. Coils were compared on the basis of signal to noise ratio (SNR) and P90 pulse length. It was found that medium coil of wire with 3 number of turns has the biggest SNR of 177 which is good for NMR procedures. On the other hand, coil with 5 numbers of turns has the shortest P90 pulse length of 2.0 μs which is good for spatial resolution. At all rate, this research have shown how theories are verified through experiment.

Keywords: GARField MRI; tune and match capacitor; CPMG; stray capacitance; signal to noise ratio.

1. INTRODUCTION

The conventional Magnetic Resonance Imaging (MRI) has been developing since 1973 [1]. Current research is carried out in the area of medical physics and diagnosis and is focused on finding 3-D anatomical images. These are now routinely obtained. One of the major considerations is for these images to show high contrast in the presence of other tissue types based on parameters such as nuclear spin relaxation times T_1 and T_2. However, only rarely are these parameters measured accurately and quantitatively from the images. One dimensional measurement is more often used in materials science application of MRI because there is no fundamental value in obtaining three dimensional images. Therefore, to obtain better spatial localisation to analyse either the sample or sample process, one would result to quantitative measurements in one dimension. In materials science, the relaxation times are wanted and measured in 1-D more accurately. Planar samples are adequately characterised with 1-D profiling. Different design of MRI magnets have been employed to study planar systems and they always have one thing in common: A spatial varying magnetic field to provide resolution in 1-D. The stable magnetic field gradients are suitable for planar imaging and are related to stray-field of magnets, whether electromagnets, superconducting coils or permanent magnetic substance.

In the later 1980s and early 1990s, STRAY Field Imaging (STRAFI) [2] was one of the methods used to routinely and reliably provide profiles and images of solid samples. Samples can be profiled with resolution on the order of a few micrometres to a few tens of micrometres. However, its application to planar samples is limited since the curvature in the magnetic flux across the region of interest in STRAFI experiment limits the maximum obtainable resolution. The spatial resolution in a STRAFI is given by:

$$\Delta r = \frac{\Delta \omega_p}{\gamma G} \tag{1}$$

Where γ is the gyromagnetic ratio of the nucleus under investigation, and *G* is the gradient of magnetic fields in the z-direction and usually parallel to polarizing field B_o, with range values $G = 50 - 100$ Tm^{-1} [3].This set-back was the major reason a permanent magnet was designed to give high resolution profiles of planar samples [4]. This magnet was named GARField (Gradient At Right Angles to the Field). It employs the concepts of STRAFI and was later improved.

GARField has been used to build profiles through planar samples such as paints [4] and skin [5] with a resolution as high as 5 μm. A second GARField was introduced [6] to enable large sample profiling and used *in vivo* in imaging of human skin [3].

In addition to that, measurement of NMR signals from planar volume-slices near to the surface of large samples becomes possible. This could either be profiling of too large samples such as building concrete [7] or trees. Unsuitable [e.g. ferromagnetic substances [8] to be inserted into a conventional MRI system offers a different set-back which has been overcome by unilateral NMR magnets. A good example of this type of system is the NMR Mobile Universal Surface Explorer (NMR-MOUSE) [9]. It is basically constructed to perform *in-situ* investigations of rubber products (e.g. car tyres). The fundamental NMR-MOUSE is able to examine a few millimetres deep into the surface of a sample and now makes it possible to study water build-up behind frescoes in old churches [10].

1.1 Problem Statement

Several experiments have been conducted to reduce the unwanted sound produced during an NMR procedure which is unhealthy to patient and their relatives. This research attempts to produce resonating coils (through experiments) in an NMR machine that will generate less noise by using GARField spectrometer.

1.2 MRI Scanner

One of the most important parts of a MRI Scanner is the resonator. It consists of a coil of wire that acts as an inductor, a tuning capacitor and a second capacitor to match the electrical impedance to the spectrometer amplifiers. The theory of resonator is well established and easily understood but, in reality several practical factors make the optimum design difficult to determine [11]. Hence, this project is to build resonators of varying design for a GARField MRI system.

GARField resonators are planar in design as opposed to more common solenoidal. They require very short NMR pulse length and high bandwidth at the expense of more usual uniform excitation field. Parameters to vary include the number and spacing of the turns, the wire diameter (that affects resistance) and whether a series-parallel or parallel-series circuit is chosen.

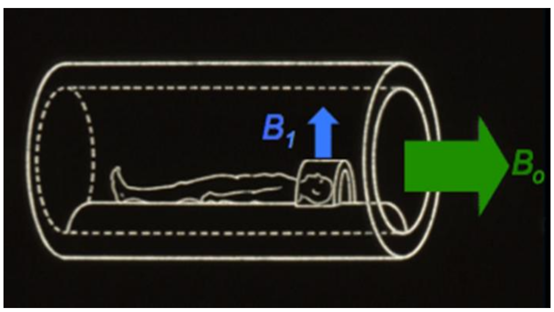

Fig. 1. The B1 RF-field is perpendicular to Bo (reproduced after [12])

A schematic of a medical system with large solenoid magnet for B_o and a head RF coil for $B_1$for head imaging is shown in Fig. 1.1. Note B_1 must be orthogonal to B_o.

2. MATERIALS AND METHODS

2.1 Materials

Bravo Impedance Meter, Spectrum Analyser (HF 2025E).

2.2 Methods

The requirement for GARField as a coil of diameter about $10-20$ mm and length $5-15$ mm tuned to frequency of $23-23.4$ MHz at $50\,\Omega$ is as follows.

The design of coils commences by ensuring the required Perspex tube was in place and with cut spiral spacing. The Presence of the cut spiral spacing of 0.2 mm (to wind coils on) allows the coil to easily align (i.e., to ensure that the centre of the wire was positioned in the same direction for each coil [13] in the same direction without closing one another). Coils were made with different numbers of turns (3, 5, and 7) and different wire thicknesses. This was followed by taking measurements of the diameter of each wire, with the thin wire having a diameter of (0.20 ± 0.01)mm, medium having a diameter of (0.45 ± 0.01) mm and thick wire with diameter(1.25 ± 0.01) mm, respectively. These different sizes of wire were considered in other to determine the variation of resistance as the diameter changes from thin to thick. Furthermore, a masking tape was used to hold the copper coil of wire end points to about a 15 mm diameter Perspex tube and the wire was then tightly wind on the spiral groove on the Perspex tube to the required number of turns and taping over it when finished, so it does not unwind. In addition to this, the terminals of the end of the coil of wire was taking out through a tiny hole on the Veroboard and it was then soldered. This was done to ensure firm connection of the terminals on the Veroboard. The Veroboard has a dimension of (40 ± 0.01) mm x (60 ± 0.01) mm. The Perspex tube was inserted via a bigger hole (inscribed on the Veroboard) with diameter equals to that of the Perspex tube, respectively. Each Perspex tube were labelled with the corresponding number of turns written on the surface of the tube for easy identification. After winding the wire and ensuring that the terminals are well soldered on the Veroboard, the capacitors were soldered in their appropriate position by considering the type of circuit to be build. In this report, the parallel-series circuit was considered in the design. The two capacitors used are C_T (tune capacitor) and C_M (match capacitor) as shown in the Fig. 2.

The C_T capacitor has fixed capacitance while C_M with a variable capacitance. The function of the C_M is to match the impedance of the coil to the electronic devices [14]. Since the target frequency is 23.4 MHz, C_T was initially connected in parallel to the output terminals of the built circuit. The frequency was then measured using the Bravo impedance meter. Several measurements were taken and each time C_T was varied until a desirable frequency was obtained which in turns gives the target frequency. At this point, the frequency read out from Bravo Impedance meter (f_Bravo) were read and recorded (see Fig. 3). The inductance in the circuit was then calculated using equation 2.

$$L = \frac{1}{(2\pi f_o)^2 C_T} \quad (2)$$

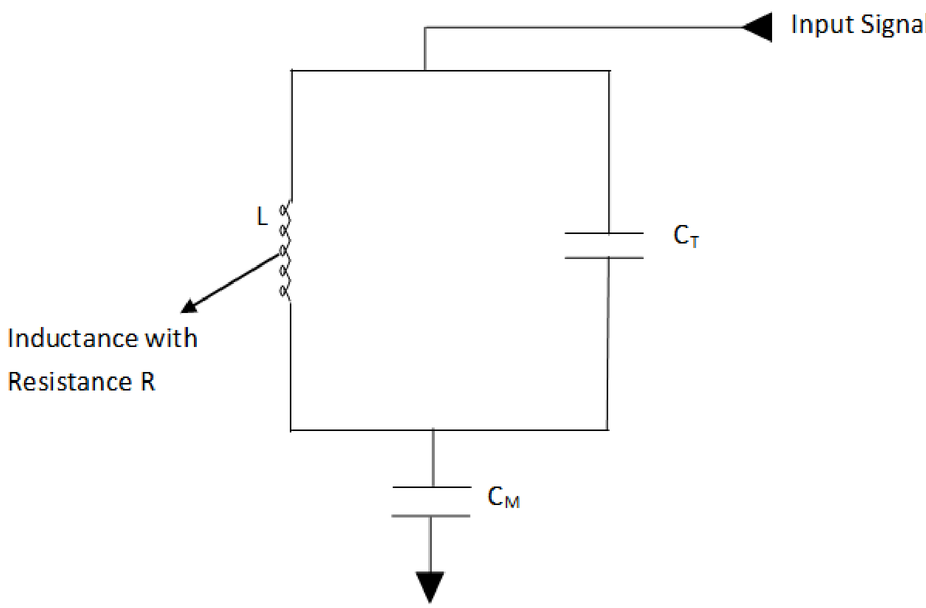

Fig. 2. Series-parallel tank circuit

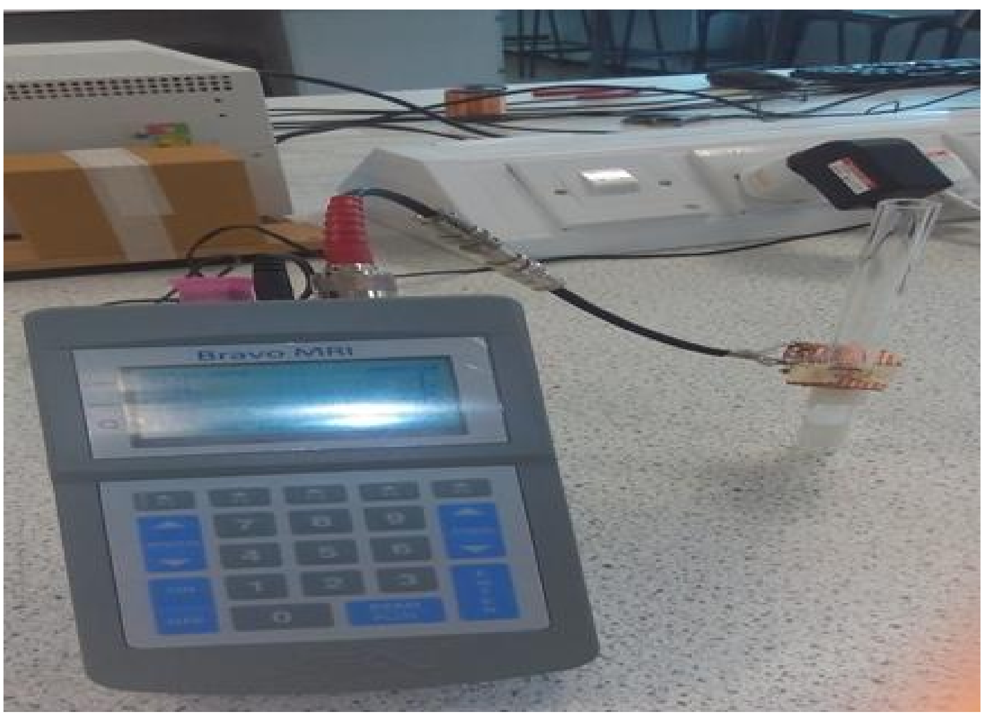

Fig. 3. Bravo connection

3. RESULTS AND DISCUSSION

Solenoid coils which have frequency with a turning range of 22-23.4 MHz were built to match total impedance at 50 Ω of a GARField. This was carried out using two capacitors (C_M and C_T) as previously explained in methods. The inductance for the 5 turns coil of wire was calculated from equation 2. This was carried out by connecting a suitable capacitor of known value in parallel with the unknown inductor creates a resonant circuit. The reflected power from the circuit arrangement displayed on the spectrum analyser was used to find the resonance frequency. The result was found to be 23.4 MHz. Different set of mica capacitors of fixed values, say, 1, 5, 10, 15, 45, 75, 100, and 200 pF were put in place for making the resonant circuit. This was followed with the use of a match capacitor to match the impedance of the circuit to the required impedance at 50 Ω. As soon as the resonance was found and knowing that the C_T for the 5 turns of coil of wire was 9.68E-11 pF, the inductance for the coil was therefore calculated using equation 2. The result for the inductance was found to be 5.64E-07 μH. However, it was found that this inductance does not give the expected result when the theoretical and experimental data were compared as they both did not agree. This was attributed to the extra inductance in the circuitry.

3.1 Inductance Estimation

Rosa and Cohen, [15], give results of L (inductance) for coils of different size. The results are complicated. There is no easy result for a short coil of a small number of turns.

Reference [$*$] which is a website, allows an approximation to be made. It requires entry of number of turns, N; length, l; radius, r of the coil. It uses the formulae given by, L $\approx \frac{\mu N^2 A}{l}$.

A second website [$**$] makes a slightly different approximation with almost similar input parameters. It uses the formulae given by, L$\approx \frac{10\pi\mu_o N^2 r^2}{9r+10L}$.These websites have been used to estimate L for coils built in this work. See Table 1.

From Table 1, it can be seen that two approximations are different and are typically smaller than the experiment. Hence, L does not depend much (if at all) on the wire thickness. In the same vein, Rainey et al., [16], in a paper titled "Estimation and measurement of flat or solenoidal coil inductance for radiofrequency NMR coil design", reported that the use of different wire materials or shape does not significantly affect the inductance of an NMR coils at high NMR frequency. These coils are at low NMR frequency. They further stated that, reference [$*$] which is a formulae frequently encountered for inductance calculation, again, does not provide a consistent estimation of inductance in the system of NMR solenoidal coils.

$*$http://hyperphysics.phy-astr.gsu.edu/hbase/electric/indsol.html [17]
$**$http://www.pulsedpower.eu/toolbox/toolbox_inductances.html [18]

3.2 Results for Impedance at 50 Ω from Experimental Plot

Fig. 4 shows the results obtained from a 5 turns coil of wire. It can be seen that the impedance goes to maximum at 23.84 MHz and minimum (phase= 0) at 23.4 MHz.The minimum frequency at 23.4 MHz corresponds to 50 Ω impedance as expected. This impedance at 50 Ω is a requirement in order to properly match to the impedance of GARField spectrometer.

Table 1. Comparison between measured inductance and literature estimated inductance values

Thickness of wire (mm)	N	l (cm)	r_{coil} (mm)	L [$*$] (μH)	L [$**$](μH)	L measured(μH)
Thin	3	0.5	7.5	0.399	0.028	2.92
Medium	3	0.5	7.5	0.399	0.028	2.80
Thick	3	0.5	7.5	0.399	0.028	2.85
Thin	5	0.7	7.5	0.793	0.075	5.78
Medium	5	0.7	7.5	0.793	0.075	5.64
Thick	5	0.7	7.5	0.793	0.075	5.25
Thin	7	1.2	7.5	0.907	0.137	8.80
Medium	7	1.2	7.5	0.907	0.137	8.90
Thick	7	1.2	7.5	0.907	0.137	11.7

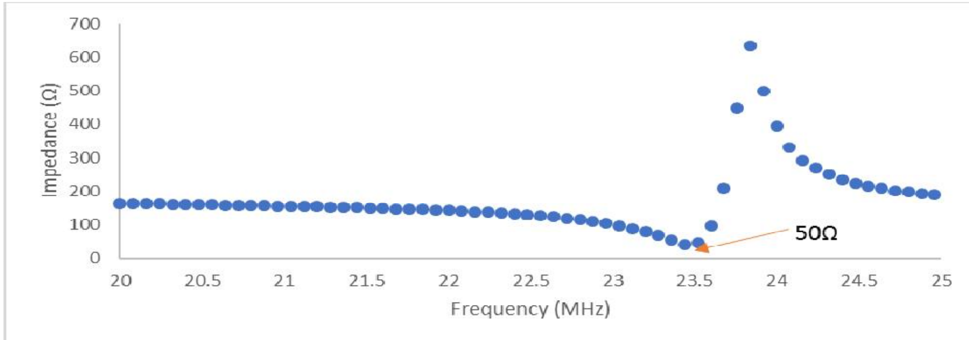

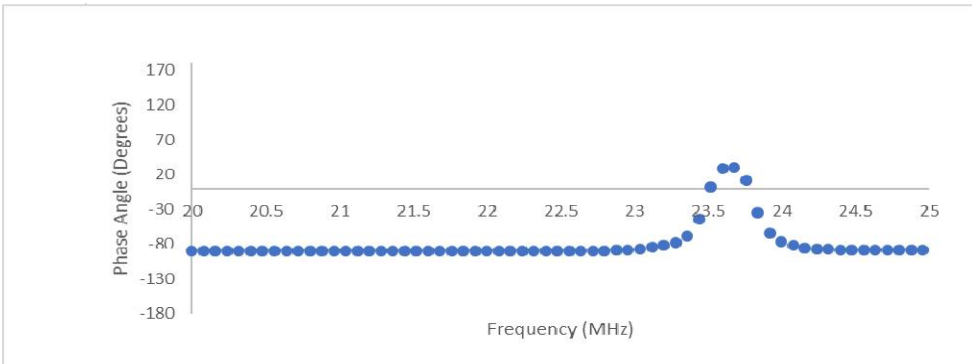

Fig. 4. Frequency vs. Phase angle for the coil with 5 turns

3.3 Results of the MATLAB Code Showing the Comparison between Theoretical and Experimental Data

MATLAB code was used to calculate the impedance and phase angle of equation 2.11. The code also read in experimental data from BRAVO.csv file and plots the experimental data on the same figure. This code was used to produce Fig. 5(a) for the coil with 5 numbers of turns (see MATLAB script in Appendix 1). The blue dotted line represents the theoretical plot for the frequency against phase angle while the solid line represents the experimental plot of frequency against phase angle, respectively. It can be seen that both frequency and phase started at the same minimum point at 23.4 MHz and increases to maximum at 23.84 MHz with a slight variation and finally drops to minimum as expected. Similarly, Fig. 5(b) shows the plot of frequency against impedance. However, in this case, it can be seen that the theoretical plot does not agree with the experimental plot. This is because neither the two plots meet at minimum nor maximum points. However, the theoretical plot (Red dotted line) is stillwell defined on the plot which is an indication that the theory still work. This large variation of experimental data not fitting with the theoretical data as we expected might be as a result of extra resistance in the coil added to the circuitry by the cabling, it could be due to capacitance arising from the inductor or stray capacitance in wire and leads. This difference could also have resulted from the fact that same inductance measured at different frequencies give slightly different values due to the distributed capacitance of the inductor. Therefore, a STRAY capacitor was used to overcome this challenge. This will be introduced shortly.

3.4 Calculation of Q-dip

Fig. 6 shows the result for the transmitted power for a coil with 5 number of turns. It can be seen that the minimum point on the reflected power corresponds to resonance frequency (f_o) at 23.4 MHz as expected. The Q-dip from the transmitted power was found by applying two methods. The first method was measuring width of the resonant power curve at half maximum (50%). Whereas the second method involve measuring the Q-dip one division below the base line level (i.e., Q-dip at 10 dB). Therefore, the Q-dip at 50% was found to be 123.7 ± 0.1 and 42.7 ± 0.1 for the Q-dip at 10dB, respectively.

The results obtained indicate that the method of $Q^{50\%}$ gave an approximate range of value (123.7 ± 0.1) expected in other to obtained total impedance at 50 Ω for the circuit. This is because the higher the Q-dip, the sharper the resonance, and the better the coil is tuned. Hence, this method was accepted on this ground.

The results obtained from the nine different coils of wire do not show a regular pattern or trends in terms of what was expected (see Table 2). It was expected that the Q-dip increases with increase in diameter and the higher the Q-dip the lower the total resistance (impedance) in the circuit. This could be attributed to extra resistance that exist between two neighbouring wires. It could even be due to the extra wire used as extension from the circuit to the spectrum analyser. However, when this result was compared to that of the theory, it shows that the coil with 7 turns of thick wire has the maximum Q-dip as expected. Also, the coil with 5 turns of wire has a relatively good Q-dip at 50% which also corresponds to resonance frequency at 23.4 MHz. Table 3 shows the design parameters used in this research. It can be seen that $C_M \ll C_T$ which does not agree with the theory for the requirement of resonance condition ($\omega_o{}^2 L C_M = 1$) to occur. However, the resistance decreases with increase in thickness of wire with thick coil of wire having less resistance as expected. This is important in other to allow sufficient power transmission with less dissipation of energy during impedance matching in the circuit design.

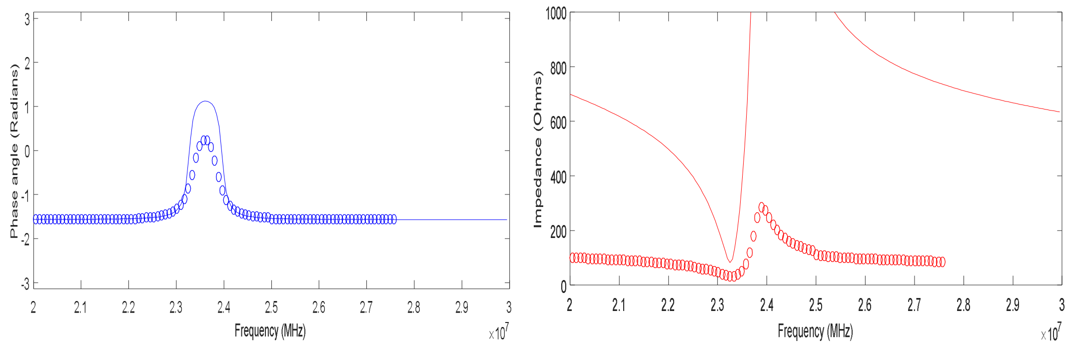

(a) (b)

Fig. 5. Frequency vs. Phase angle for the coil with 5 number of turns

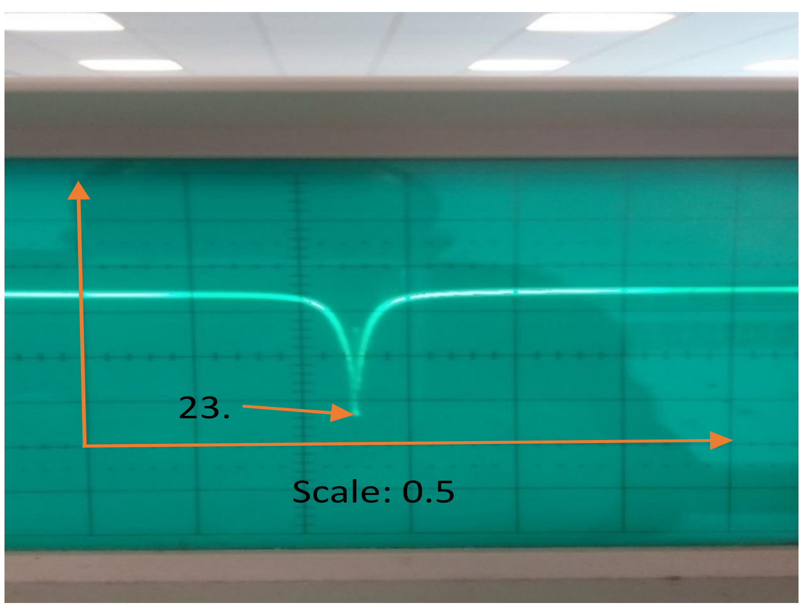

Fig. 6. Reflected power displayed for a 5 turns coil of wire observed from a spectrum analyser

Table 2. Showing the calculated and theoretical Q-values of the nine different coils with different numbers of turns (3, 5, and 7) and different wire thicknesses.

Number of Turns	Coil type	Diameter of wire (mm)	Size of wire(m)	Q_dip at 50%	Q_10 db	Q_theory
3	Thin	0.20	Thin	156	58.0	163
3	Medium	0.45	Medium	66.60	33.3	390
3	Thick	1.25	Thick	117.00	39.0	1040
5	Thin	0.20	Thin	93.60	52.0	195
5	Medium	0.45	Medium	123.70	42.7	475
5	Thick	1.25	Thick	78.00	52.0	110
7	Thin	0.20	Thin	67.14	27.6	212
7	Medium	0.45	Medium	117.00	42.5	533
7	Thick	1.25	Thick	117.00	39.0	1760

Table 3. Showing values for the design parameters

Number of Turns	Coil type	Diameter of wire (mm)	C_M (pF)	C_T (pF)	L (μH)	R (Ω)
3	Thin	0.20	20.50 ± 3.6	171.00	0.29	0.26
3	Medium	0.45	17.70 ± 3.6	212.00	0.28	0.11
3	Thick	1.25	15.30 ± 3.6	212.00	0.29	0.04
5	Thin	0.20	13.60 ± 3.6	85.00	0.58	0.44
5	Medium	0.45	16.00 ± 3.6	96.80	0.56	0.18
5	Thick	1.25	12.40 ± 3.6	105.00	0.53	0.07
7	Thin	0.20	11.60 ± 3.6	55.00	0.88	0.61
7	Medium	0.45	9.43 ± 3.6	61.00	0.89	0.25
7	Thick	1.25	8.53 ± 3.6	54.00	0.12	0.10

3.5 The Stray Capacitance

It is seen that theory does not agree with experiment. However, good results were obtained when an extra capacitor C_{STRAY} was included in the circuitry (see Fig. 7).

The modified new equation for the total impedance in the circuit is given by

$$\frac{1}{Z_{TOTAL}} = \frac{1}{Z_{CIRCUIT}} + \frac{1}{Z_{C_{STRAY}}} \quad (3)$$

$$\therefore Z_{TOTAL} = \frac{Z_{CIRCUIT} \times Z_{STRAY}}{Z_{CIRCUIT} + Z_{STRAY}} \quad (4)$$

$Z_{CIRCUIT}$ is calculated using equation

$$Z_{total} = \left[\frac{1}{j\omega L+R} + j\omega C_T\right]^{-1} + \frac{-j}{\omega C_M} \quad (5)$$

$$\text{For } Z_{C_{STRAY}} = \frac{-j}{\omega C_{STRAY}} \quad (6)$$

The stray capacitor can be attributed to capacitance:

(i) In the co-axial cable and /or
(ii) Capacitance between wires and leads in the circuit

From Farnell database (http://www.farnell.com/datasheets/84294.pdf.) [19] RG59 co-axial cable has capacitance of about 100 pF per meter. In this work, about 15 cm co-axial cable was used in the design which corresponds to 15 pF capacitor. But a stray capacitor with values ranging between $30-40$ pF was used to properly fit the experimental data to that of the theory. Therefore, a good fit was obtained when the stray capacitor was connected in parallel to the already built tank circuit. This fit the theory and experimental data as expected (see Table 4 for the values of the design parameters).

Therefore, in the present research, it was found that stray capacitance play an important role in the circuit design, so it was rather not neglected but incorporated in the circuit to make it work. See below, examples of graphs with good fits with the corresponding MATLAB scripts in appendix which include the value for the stray capacitor.

Examples of MATLAB code used to calculate the impedance and phase angle of equation 4.3.

The code read in experimental data from BRAVO.csv file and plots the experimental data on the same figure. This code was used to produce Figs. 8, 9 and 10, respectively.

3.6 Results for the NMR Experiments

The NMR experiment was conducted in the NMR lab. Measurements were performed using the GARField. The ^{1}H frequency is $20-30$ MHz depending on the sample position. This was targeted at 23 MHz. The gradient strength of the GARField used is 11.6 T/m at 30 MHz. The ratio of field gradient to frequency is a constant in GARField. Therefore, at 23 MHz the gradient is $\frac{23}{30} \times 11.6 = 8.9\ \mathrm{T/m}$.

Proton resolution measurements were made using a rubber solution contained in a glass test tube. The tube was placed inside the medium coil of wire with different number of turns (3, 5, 7 turns) and thickness. The entire sep-up was rigidly located in the GARField magnet with the RF coil in the centre and placed in a Faraday cage. Sample position adjustment was carried out by adjusting the positioning plate to ensure that the sample is in the right position and reproducible. CPMG NMR spectrawere acquired at this point (see Fig. 11) which shows both the real component of the signal (Blue) and imaginary componentof the signal echoes(Orange), respectively.

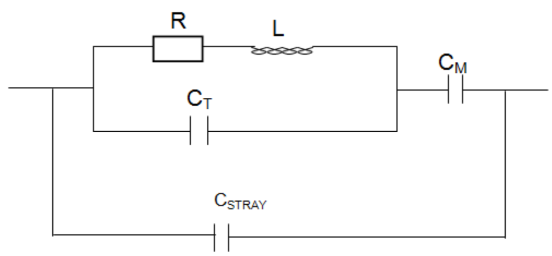

Fig. 7. Modified circuit showing the connection of stray capacitor in parallel to the already existing tank circuit

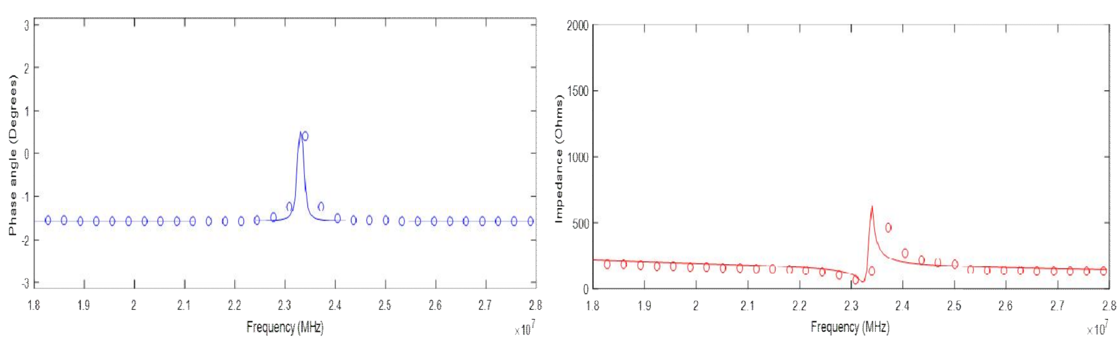

Fig. 8. Best fit obtained with Stray Capacitor for 3 turns medium coil of wire

Table 4. Fit parameters for 3, 5 and 7 turns medium coil of wire

Fit parameters for 3 turn medium coil of wire		Fit parameters for 5 turn medium coil of wire		Fit parameters for 7 turn medium coil of wire	
Parameter	**Value**	**Parameter**	**Value**	**Parameter**	**Value**
C_T	82.10 pF	C_T	85.00 pF	C_T	85.00 pF
C_M	6.4 pF	C_M	7.60 pF	C_M	8.00 pF
C_{STRAY}	33.00 pF	C_{STRAY}	40.00 pF	C_{STRAY}	32.00 pF
R	0.26229 Ω	R	0.17 Ω	R	0.24 Ω
L	0.53μH	L	0.50 μH	L	0.50 μH

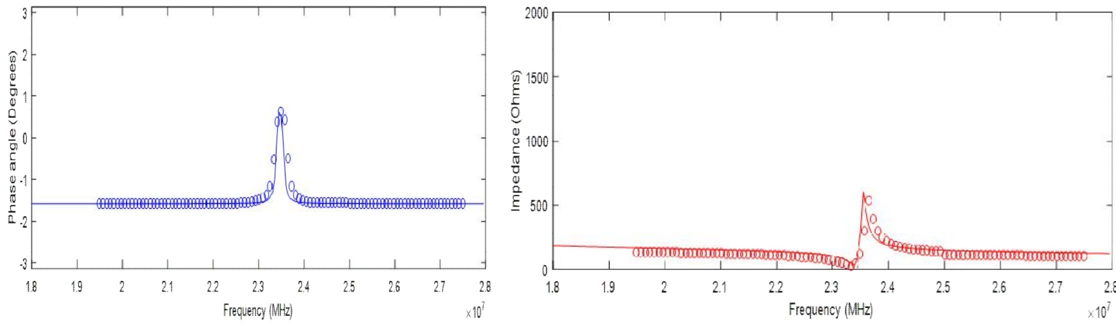

Fig. 9. Best fit obtained with Stray Capacitor for 5 turns medium coil of wire

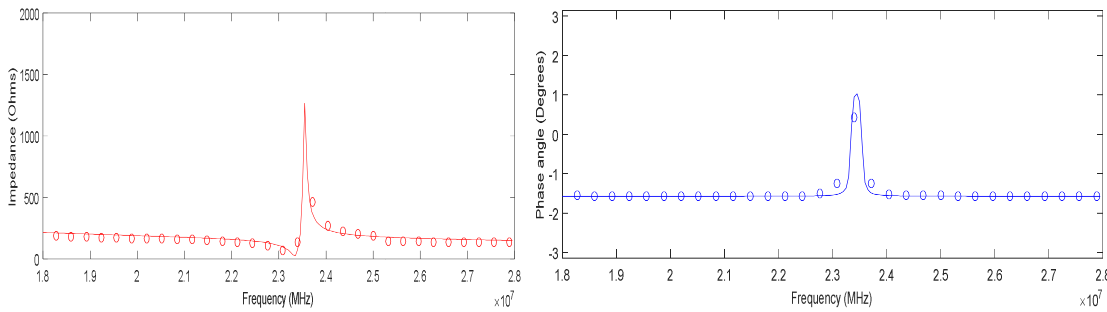

Fig. 10. Best fit obtained with Stray Capacitor for 7 turns thick coil of wire

Table 5. Showing the constant CPMG parameters

Parameter	Value
90 Amplitude	-6 dB
180 Amplitude	-0 dB
Acquired time	0.064 ms
Band width	1 MHz
Dwell time	1.0 µs
Echo time	150 µs
Experiment	CPMG
Filter	No
Number of echoes	16
Number of points	64 points per echoes
Number of scans	64 number of averages
Receiver gain	19 dB

The constant CPMG parameters are given in table 5. Note 16 echoes were acquired with 64 averages each. The frequency was changed to the coil frequency and the P90 pulse length was adjusted for maximum signal in the $2^{nd}/3^{rd}$ echoes and about 67% maximum in the 1^{st} echo. This follows procedure in reference [20].

3.7 Results for the 3 Turn Coil

The P90 pulse length was 3 µs and is given in Table 6. The results are shown in Fig. 11. The coils with 5 and 7 turns were also tested with the same parameters (Table 5) and the frequency and P90 pulse lengths found (Table 6).

Table 6. Showing the P90 pulse length and the B1 frequency for different coils

Number of turns	P90 pulse length (µs)	B1Frequency (MHz)
3	3	23.3
5	2	23.4
7	3.5	23.1

3.8 Analysis

Fig. 12 shows the results for the time plotted as a function of the magnitude of the signal. It can be seen that there are 16 echoes with the first having the lowest signal when compared with the remaining echoes as expected.

The signal to noise ratio (SNR) for the whole coils was calculated using the biggest echo signal from the spectrum shown in Fig. 12. This carried out using the equation below

$$\text{SNR} = \frac{S}{N} \quad (7)$$

Where

S is the signal given by,

$$\text{S} = \sqrt{{S_{Real}}^2 + {S_{Imaginary}}^2} \quad (8)$$

N is the noise calculated as the average value of the baseline signal.

Considering an extract of the third echo signal produced by coil with 3 number of turns as shown in Fig. 13. The SNR was calculated by taken 20 echoes points before and after the biggest signal (see Fig. 13). These 20 echoes points represent the noise in the signal. The result for these calculations is tabulated in Table 5.

3.8 Discussion

The Table 7 shows the results for the calculated signal to noise ratio. It is clear from the result that 3 turns medium coil of wire has the highest SNR of 177 followed by 7 turns medium coil with 160 SNR. Although, 5 turns coil has the lowest SNR of 150. Therefore, in terms of SNR, 3 turns coil of wire will perform better due to its biggest echoes signal to noise ratio. On the other hand, if the pulse length is considered, the 5 turns coil of wire will perform best in this regards since shorter pulse length give better resolution for scanning purposes. The pulse length is inversely proportional to the selected slice width. The shorter the pulse, the wider the excited slice and so more human tissue skin depth is seen *in-vivo*. Therefore, short pulse is best. This results indicate that wire resistance has little or no effect on the performance of the coils in general. This is because C_{STRAY} seems to dominate the coil Q and not R.

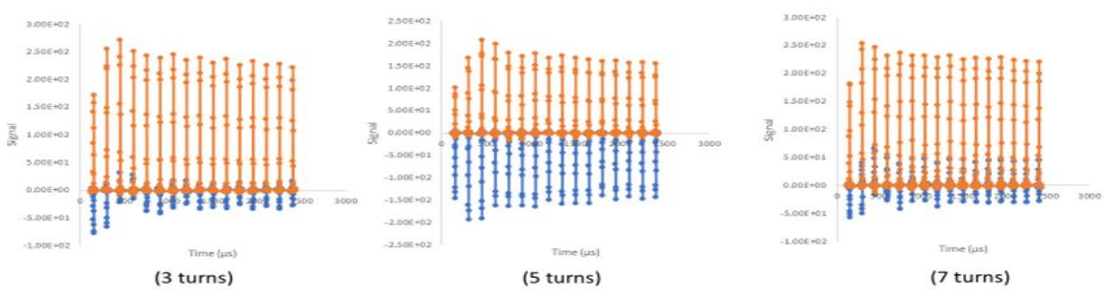

Fig. 11. Spectrum showing the real and imaginary signals for each corresponding coil

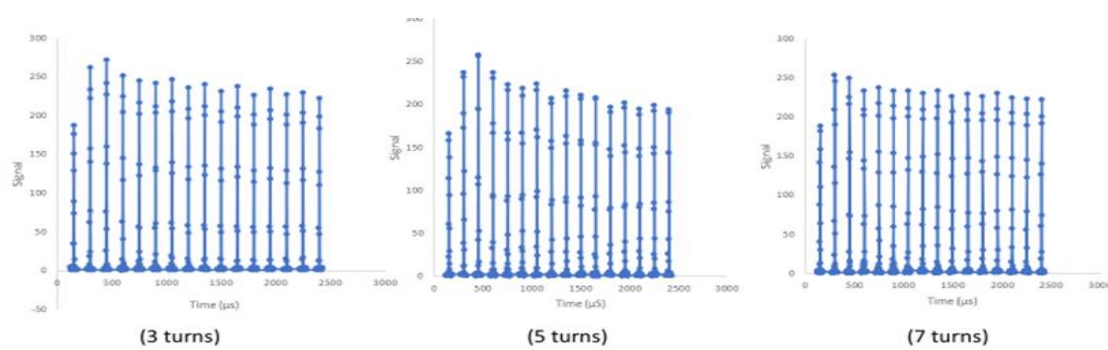

Fig. 12. NMR Signals

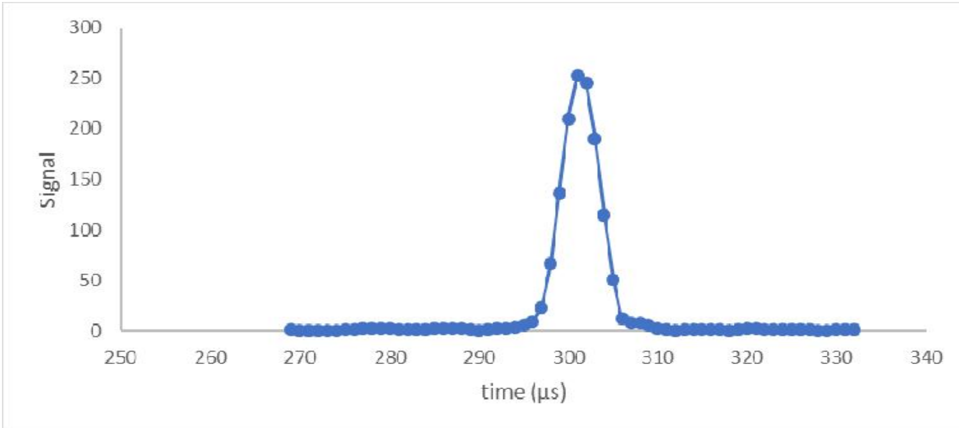

Fig. 13. 3rd echo signal from 3 turns medium coil of wire

Table 7. Showing results for the calculated SNR

Thickness of wire	Number of turns	3rd Signal echo	Noise (2nd echo)	SNR	Pulse length (µs)
Medium	3.00	260.00	1.48	177.00	3.00
Medium	5.00	236.00	1.54	150.00	2.00
Medium	7.00	250.00	1.57	160.00	3.50

4. CONCLUSION

Several experiments have demonstrated that GARField MR profiling is widely used both in medicine and industry. It is able to probe the surface of the human skin to different depths between the stratum corneum and viable epidermis of the human abdominal skin tissue *in vivo and in vitro.* In this work, nine different resonant circuit were designed with varying thickness and number of turns for a GARField system. Each of the circuit was tuned to frequency within $22 - 23$ MHz to match the spectrometer of the GARField. The quality of the coils was calculated using the Q-dip observed from the reflected power seen on the spectrum analyser and the Q-dip at 50% was found to be 123.7 ± 0.1 as expected in other to match the total impedance at 50 Ω to the spectrometer of the GARField. However, the resistance was found to have little or no effect in all the coils.

Three medium coils were tested in the NMR laboratory using a GARField spectrometer to determine the best coil that could be applied for NMR experiment. Two parameters were considered for this purpose. The SNR and P90 pulse length. The coil with 3 number of turns has the biggest SNR of 177 (which is good for NMR experiment) and coil with 5 number of turns was found to have the shortest P90 pulse length of about 2.0 µs which is good as well. Therefore, medium coil of wire with 3 and 5 number of turns will perform better for NMR/MRI procedure based on the Secriteria's (SNR and P90 pulse length).

COMPETING INTERESTS

Authors have declared that no competing interests exist.

REFERENCES

1. Mitchell J, Blumber P, McDonald PJ. Spatially resolved nuclear magnetic resonance studies of planar samples. Progress in Nuclear Magnetic Resonance Spectroscopy; 2006.
2. Samoilenko AA, Artemov DY, Sibeldina LA. Jetp Lett. 1988;47:417.
3. McDonald PJ, Akhmerov A, Backhouse LJ, Pitts S. Magnetic resonance profiling of human skin *in vivo* using GARField magnets. J Pharm. Sci. 2005;94: 1850. Magnetic Resonance Profiling of Human Skin in Vivo using GARField Magnetys. Journal of Pharmaceutical Sciences. 2005;94.
4. Glover PM, Aptaker PS, Bowler JR, Ciampi E, McDonald PJ J. Magn. Reson. 1999;139:90.

5. Backhouse L, Dias M, Gorce JP, Hadgraft J, McDonald PJ, Wiechers JW. J. Pharm. Sci. 2004;93:2274.
6. Bennett G, Gorce JP, Keddie JL, McDonald PJ, Berglind H Magn. Reson. Imaging. 2003;21:235.
7. Sharma S, Casanova F, Wache W, Segre A, Blumich B. Magn. Reson. Imaging. 2003;21:249.
8. Zimmer G, Guthausen A, Schmitz U, Saito K, Blumich B. Adv. Mater. 1997;9:987.
9. Eidmann G, Savelsberg R, Blumler P, Blumich B. J. Magn. Reson. Ser. A. 1996;122:104.
10. Purcell EM. Electricity and magnetism: Berkeley physics course-Volume 2. New York: McGraw-Hill; 1985.
11. Fukushima E, Roeder SBW. Experimental pulse NMR: A nuts and bolts approach. Addison-Wesley, New York. 1981;407-415.
12. Klomp D, Koning W, Hoogduin H, Raaijmakers A, Petridou N, Vande Berg N, Luijten P. Practical design of RF transmit and receive arrays. ESMRMB; 2011.
13. Viqueira WD, Berger W, Robles JP, Santyr GE. Litz wire radiofrequency receiver coils for hyperpolarized noble gas MR imaging of rodent lungs at 73.5 Mt. Concepts MagnReson Part B (MagnReson Engineering). 2010;37B(2):75-85.
14. Pollak L, Slater RR. Input circuits for pulsed NMR. Rev. Sci. Instrum. 1966;37: 268-272.
15. Rosa EB, Cohen L. The mutual inductance of coaxial solenoids. Cayley, Elliptic functions. 1907;139.
16. Rainey JK, DeVries JS, Sykes BD. Estimation and measurement of flat or solenoidal coil inductance for radiofrequency NMR coil design. Journal of Magnetic Resonance. 2007;187:27-37.
17. Available:http://hyperphysics.phy-astr.gsu.edu/hbase/electric/indsol.html
18. Available:http://www.pulsedpower.eu/toolbox/toolbox_inductances.html
19. Available:http://www.farnell.com/datasheets/84294.pd
20. McDonald PJ, Newling B. Rep. Prog. Phys. 1998;61: 1441.

APPENDIX 1

```
N=200; % size of vectors : number of frequencies to calculate
Ct=9.68E-11; % tune capacitor in pF
Cm = 1.62E-11;  % match capacitor in pF
L=5.64E-07; % inductance
% Wire and coil
n=5; % number or turns
dia = 1.44e-2; % diamter of coil in m
l=n*pi*dia; % length of wire
d=0.00045; % diameter of wire in m
rho=1.7e-8; % resistivity of Cu in Ohm metere
delta=14e-6; % skin depth of copper - thickness of surafce layer in which current
flows
R=(l*rho)/(pi*d*delta); % resistance of wire
['Resistance = ',num2str(R),' Ohms'] % Prints Resistance
f1=20e6; % minimum frequency to test
f2=30e6; % maximum frequency to test
df=(f2-f1)/N; % frequency step

f=zeros(N,1); % declare an array of size N by 1 for f and sets to zero
zL=zeros(N,1); % same for impedance of L
zCm=zeros(N,1); % same for impedance of Cm
zCt=zeros(N,1); % same for impedance of Ct
```

```
z=zeros(N,1); % same for total impedance

for i=1:200   % sets all the f values
   f(i)=f1+(i-1)*df;
end
   zL=1j*2*pi*f*L+R; % calculate zL
   zCt=1./(1j*2*pi*f*Ct); % calculate zCt. Use ./ for array division
   zCm=1./(1j*2*pi*f*Cm); % calculate zCm.
Use ./ for array division
   %z=1./((1./(zL+zCt))+(1./zCm)); %formulae for series-parallel
   z=1./((1./zL)+(1./zCt))+zCm; %calculate z total formulae for parallel - series
   phase=atan2(imag(z),real(z)); %calcuate phase angle total

% Get measured data

Data=csvread('5_T_medium.csv');
Data_Impedance=Data(:,5); %reads colum 5 of data
Data_Freq=Data(:,2)*1e6;
Data_Phase=Data(:,7)*pi/180;
  figure(1); % plot two figures
  plot(f,abs(z),'-r');
  hold on
  plot(Data_Freq(:),Data_Impedance(:),'or');
  hold off
  xlim([f1,f2]);
  ylim([0,1000]);
  title('impedance in ohms')
  grid on
  figure(2);
  plot(f,phase,'-b');
  hold on
  plot(Data_Freq(:),Data_Phase(:),'ob');
  hold off
```

```
xlim([f1,f2]);
ylim([-pi,pi]);
title('phase in radians')
grid on
```


Peer-review history:
The peer review history for this paper can be accessed here:
http://www.sdiarticle4.com/review-history/66731